

## Dark production of hydrogen peroxide in the Gulf of Alaska

Andrew W. Vermilyea,<sup>1</sup> S. Paul Hansard, and Bettina M. Voelker\*

Colorado School of Mines, Department of Chemistry and Geochemistry, Golden, Colorado

### Abstract

Dark H<sub>2</sub>O<sub>2</sub> production rates were measured in samples collected in the Gulf of Alaska. We used a simple, novel method for determining absolute rates of dark production and decay of H<sub>2</sub>O<sub>2</sub>, both of which are occurring simultaneously (presumably as a result of biological activity) in unfiltered samples. [H<sub>2</sub>O<sub>2</sub>] vs. time was measured in 24-h dark incubations of both unaltered samples and the same samples spiked with 100–250 nmol L<sup>-1</sup> H<sub>2</sub>O<sub>2</sub>. Data were modeled with zero-order H<sub>2</sub>O<sub>2</sub> production rates and first-order H<sub>2</sub>O<sub>2</sub> decay coefficients as fitting parameters, with the assumption that addition of [H<sub>2</sub>O<sub>2</sub>] to a sample does not change either parameter. H<sub>2</sub>O<sub>2</sub> production rates ranged from < 0.5 nmol L<sup>-1</sup> h<sup>-1</sup> to 8 nmol L<sup>-1</sup> h<sup>-1</sup>, and generally decreased with depth and decreasing chlorophyll. Comparison of dark production with estimates of average photochemical H<sub>2</sub>O<sub>2</sub> production rates in the top 50 m of the water column indicated that dark production is likely to be a significant source of H<sub>2</sub>O<sub>2</sub>. Indeed, many of the unaltered incubations indicated that in situ [H<sub>2</sub>O<sub>2</sub>] was close to a steady state between dark production and decay, especially in samples from depths of ≥ 10 m.

The reactive oxygen species hydrogen peroxide (H<sub>2</sub>O<sub>2</sub>) and superoxide (O<sub>2</sub><sup>-</sup>) are intermediates formed during the sequential one-electron reduction of O<sub>2</sub> to H<sub>2</sub>O. Thanks to recently developed techniques allowing direct detection of O<sub>2</sub><sup>-</sup> in marine water samples (Rose et al. 2008a,b), interest is growing in its role as a reductant or oxidant of redox-active trace metals in the ocean. Reactions with H<sub>2</sub>O<sub>2</sub> have also been suggested to be important to the marine redox cycling of Cu (Moffett and Zika 1987), Fe (Moffett and Zika 1987; Millero and Sotolongo 1989), Mn (Sunda and Huntsman 1994), and Cr (Pettine et al. 2008).

Because H<sub>2</sub>O<sub>2</sub> is much more stable and, therefore, easier to measure than O<sub>2</sub><sup>-</sup>, a substantial body of work already exists regarding H<sub>2</sub>O<sub>2</sub> sources and sinks in the marine environment. The major decay process is particle-associated, and thought to be catalysis of H<sub>2</sub>O<sub>2</sub> dismutation or reduction by microorganisms that contain catalases and peroxidases (Moffett and Zafiriou 1990; Cooper et al. 1994; Wong et al. 2003). H<sub>2</sub>O<sub>2</sub> formation is traditionally attributed to photo-oxidation of chromophoric dissolved organic matter (CDOM) by molecular oxygen, to produce the superoxide radical anion, O<sub>2</sub><sup>-</sup> (Petasne and Zika 1987; Micinski et al. 1993). It is then assumed that dismutation of O<sub>2</sub><sup>-</sup> occurs, leading to 1 mol of H<sub>2</sub>O<sub>2</sub> per 2 mol of O<sub>2</sub><sup>-</sup>. Near-surface photochemical production rates of H<sub>2</sub>O<sub>2</sub> can be much higher in coastal waters where CDOM concentrations are high (4–300 nmol L<sup>-1</sup> h<sup>-1</sup>), as compared to the open ocean (2–15 nmol L<sup>-1</sup> h<sup>-1</sup>; Table 1). Table 1 includes data from both filtered and unfiltered irradiations, giving absolute and net H<sub>2</sub>O<sub>2</sub> photochemical production rates, respectively. The rates determined in either type of irradiation should be similar, because during short irradiation times dark decay is small compared to photochemical production. Yuan and Shiller (2001) observed similar rates

of H<sub>2</sub>O<sub>2</sub> photoproduction for unfiltered and 0.4-μm filtered irradiations.

There is growing evidence that biological production could also be an important source of H<sub>2</sub>O<sub>2</sub>. Production of O<sub>2</sub><sup>-</sup>, which presumably results in H<sub>2</sub>O<sub>2</sub> just as it does in the photochemical pathway, has been observed in cultures of several phytoplankton species including the red tide organism *Chattonella marina* (Kim et al. 2000), marine diatoms *Thalassiosira weissflogii* and *Thalassiosira pseudonana* (Kustka et al. 2005), the cyanobacterium *Lyngbya majuscula* (Rose et al. 2005), and many of the 37 species of marine microalgae surveyed by Marshall et al. (2005). H<sub>2</sub>O<sub>2</sub> production via a pathway that does not involve O<sub>2</sub><sup>-</sup> as an intermediate has also been measured, in cultures of *Hymenomonas carterae* (Palenik et al. 1987). Furthermore, initially present H<sub>2</sub>O<sub>2</sub> decayed toward nonzero steady-state concentrations in dark incubations of some unfiltered water samples from the Mediterranean Sea (Herut et al. 1998), suggesting simultaneous decay and production. Overnight in situ H<sub>2</sub>O<sub>2</sub> concentrations also approached a nonzero steady state in both the Atlantic (Yuan and Shiller 2001; Avery et al. 2005) and the Pacific (Yuan and Shiller 2005). Avery et al. (2005) claimed this [H<sub>2</sub>O<sub>2</sub>]<sub>ss</sub> was due to H<sub>2</sub>O<sub>2</sub> from rain and air mixing with surface water; however, biological production could also play a role. Recently Yuan and Shiller (2004) have measured H<sub>2</sub>O<sub>2</sub> concentrations up to 6 nmol L<sup>-1</sup> at 5000 m and proposed a biological origin due to the short half-life of H<sub>2</sub>O<sub>2</sub> compared to transport times of photochemically produced H<sub>2</sub>O<sub>2</sub> to such depths. It has also been proposed by Yuan and Shiller (2005), after observing a diurnal cycle on only 1 d during a month-long cruise from Japan to Hawaii, that biological H<sub>2</sub>O<sub>2</sub> production may control the in situ concentrations measured in the Northwest Pacific. Net dark production of H<sub>2</sub>O<sub>2</sub> has been observed in unfiltered samples from the Sargasso Sea (Palenik and Morel 1988). Finally, Moffett and Zafiriou (1990) showed that decay of isotopically labeled H<sub>2</sub>O<sub>2</sub> was faster than decay of unlabeled H<sub>2</sub>O<sub>2</sub> in dark incubations of unfiltered coastal

\* Corresponding author: voelker@mines.edu

<sup>1</sup> Present address: University of Alaska Southeast, Environmental Science Program, Juneau, Alaska

Table 1. Hydrogen peroxide photochemical production rates for various marine studies.

Study location	H <sub>2</sub> O <sub>2</sub> photoformation rate (nmol L <sup>-1</sup> h <sup>-1</sup> )	Reference
Open ocean		
Antarctic waters, surface	2.1–9.6*	(Yocis et al. 2000)
Bermuda (BATS), surface	2.2–9.4†	(Avery et al. 2005)
Central Atlantic	5.5†	(Obernosterer et al. 2001)
Central Atlantic	8.3‡, 5.4§, 15	(Yuan and Shiller 2001)
NW Pacific	8‡	(Yuan and Shiller 2005)
Coastal waters		
Caribbean Sea	23.6–134‡	(Moore et al. 1993)
Mediterranean coast	38–304*‡	(Herut et al. 1998)
Red Sea coast	40–60*‡	(Herut et al. 1998)
Baltic Sea coast	3.6–183*‡	(Herut et al. 1998)
Mediterranean Sea	9.0‡	(Johnson et al. 1989)
Mediterranean coast, surface	67‡	(Price et al. 1998)

\* 0.2  $\mu\text{m}$  filtered.

† Measured in situ with [H<sub>2</sub>O<sub>2</sub>] measurements over the day.

‡ Unfiltered.

§ 0.4- $\mu\text{m}$  filtered.

|| Ultrafiltered.

water samples, and concluded that H<sub>2</sub>O<sub>2</sub> production, at absolute production rates of 0.8–2.4 nmol L<sup>-1</sup> h<sup>-1</sup>, accounted for the difference. While only the culture studies can unequivocally attribute observed O<sub>2</sub><sup>-</sup> or H<sub>2</sub>O<sub>2</sub> production to the organisms present, no alternative mechanism of dark, particle-associated production of H<sub>2</sub>O<sub>2</sub> has been suggested.

The measurement of dark H<sub>2</sub>O<sub>2</sub> production rates is complicated by the fact H<sub>2</sub>O<sub>2</sub> decay is occurring simultaneously in unfiltered samples. The goal of this study was to determine whether dark H<sub>2</sub>O<sub>2</sub> production is a significant source of H<sub>2</sub>O<sub>2</sub> to the Gulf of Alaska (GoA). To accomplish this goal, we developed a new, simple method to distinguish absolute dark production and decay rates of hydrogen peroxide from observed net rates in unfiltered samples.

## Methods

*Sampling locations and procedures*—Data were collected while aboard the R/V *Thomas G. Thompson* on a research cruise throughout the GoA between 19 August and 17 September 2007. The majority of the stations were located throughout a mesoscale eddy southwest of Kodiak Island. Additional stations were located south of Seward, Alaska (up to 320 km offshore) and WSW of Yakutat, Alaska (up to 800 km offshore). Exact coordinates of each station are provided in Vermilyea (2009). Surface samples and samples from depth were collected by two different systems, both of which emphasized trace-metal clean sampling. Surface samples (referred to as ‘fish’ samples) were collected while the ship was underway to prevent contamination from the ship itself. Seawater was pumped from about 8 m out from the side of the ship into a Class 100 clean van. Fish samples were collected at a depth of ~ 1 m during transects, except for a few deeper samples (< 10 m). Fish samples collected while on station were from a depth of ~ 10 m. Subsurface

samples (referred to as GO-FLO samples) were collected at depths of 10 m, 25 m, and 50 m using 30-liter, trace-metal clean, Teflon-lined, GO-FLO bottles on a Kevlar cable. Both fish and GO-FLO samples were filtered using 0.45- $\mu\text{m}$  acid-cleaned Teflon-membrane capsule filters (Osmonics).

GO-FLO and surface fish samples were collected for H<sub>2</sub>O<sub>2</sub> incubations, as either unfiltered samples or 0.45- $\mu\text{m}$  filtered controls, directly into acid-washed, Q-water rinsed, dark amber high-density polyethylene (HDPE) 250-mL screw-top bottles. Care was taken that the bottles were completely filled, because substantial contamination of H<sub>2</sub>O<sub>2</sub> from air could be observed if a headspace remained.

*Hydrogen peroxide analysis*—H<sub>2</sub>O<sub>2</sub> concentration was determined by the chemiluminescing reaction between acridinium ester (10-methyl-9-(p-formylphenyl)-acridinium carboxylate trifluoromethanesulfonate) and the conjugate base of H<sub>2</sub>O<sub>2</sub> (HO<sub>2</sub><sup>-</sup>, pK<sub>a</sub> 11.6; Cooper et al. 2000). The method was carried out as a flow injection analysis (Miller et al. 2005; King et al. 2007) using a FeLume system (Waterville Analytical). Briefly, a filtered seawater carrier that was prepared daily with catalase entered a 10-way injector, where it pushed a slug of filtered or unfiltered sample through a 500- $\mu\text{L}$  sample loop. The sample then mixed with the acridinium ester reagent (5  $\mu\text{mol L}^{-1}$ , pH 3), which was prepared every day or two from a refrigerated pH 3, 550- $\mu\text{mol L}^{-1}$  stock solution. The reagent-sample mixture passed through a mixing loop (1 m) and entered the flow cell located at the photo multiplier tube interface, where it mixed with a pH 11 carbonate buffer (0.01 mol L<sup>-1</sup>) to initiate the chemiluminescence-generating reaction. An acid-wash loop was integrated as previously described (Miller et al. 2005) to continually rinse the seawater precipitates formed. After every set of samples, 0.01 mol L<sup>-1</sup> HCl was run through the system for 5 min followed by 5 min of Q-water. All

solutions contained 25,000 units catalase L<sup>-1</sup> (1 mg L<sup>-1</sup>) except the samples and the acid and Q-water washes. At this catalase concentration, < 1% of the H<sub>2</sub>O<sub>2</sub> is degraded during analysis.

Standard additions of H<sub>2</sub>O<sub>2</sub> (10–200 nmol L<sup>-1</sup>) were performed every 45–60 min to obtain a calibration slope ( $R^2 > 0.98$ ), with no discernable change in sensitivity (slope) due to matrix effects from the various filtered seawater samples used. H<sub>2</sub>O<sub>2</sub> ‘blanks’ were defined as filtered seawater samples from 300 m containing 100,000 units catalase L<sup>-1</sup> (4 mg L<sup>-1</sup>) set in the dark for  $\geq 10$  min. No decrease was observed in the chemiluminescence signal of the blanks after 10 min, because this water contained very low initial [H<sub>2</sub>O<sub>2</sub>] (< 5 nM). While these blanks may contain 1 nmol L<sup>-1</sup> or 2 nmol L<sup>-1</sup> H<sub>2</sub>O<sub>2</sub> (Yuan and Shiller 1999), these values are around the detection limit of the analysis, and we never observed in situ concentrations resulting in negative peaks (implying lower [H<sub>2</sub>O<sub>2</sub>] in the sample than in the catalase-amended carrier) even in samples from 300-m depth.

*Dark incubations: Absolute rates of H<sub>2</sub>O<sub>2</sub> dark production and decay*—For any single dark incubation experiment, at least two (up to four) unfiltered samples in opaque (brown) HDPE bottles were collected, and occasionally also one filtered sample as an experimental control. One of the unfiltered samples and the filtered control were left unaltered and the remaining one to three unfiltered bottles were spiked with additional H<sub>2</sub>O<sub>2</sub>, ranging from 100 nmol L<sup>-1</sup> to 250 nmol L<sup>-1</sup> total [H<sub>2</sub>O<sub>2</sub>] for most samples. The bottles were incubated in sealed plastic bags on the ship-deck with surface seawater constantly circulating around them (8.5–18°C), and aliquots were withdrawn for H<sub>2</sub>O<sub>2</sub> measurement five to six times over the next 24 h. After each aliquot was withdrawn, bottles were squeezed and then recapped tightly, so that no headspace remained, minimizing the possibility of H<sub>2</sub>O<sub>2</sub> contamination from the air. Each bottle was shaken prior to sampling, but with no headspace, mixing may have been minimal and probably contributed a small amount of error to individual [H<sub>2</sub>O<sub>2</sub>] measurements.

*Photochemical production*—Ship-deck irradiations of both filtered and unfiltered samples were carried out for 10-m samples from two stations on 22 and 23 August 2007, under mostly sunny skies from 15:00 h to 19:00 h local time on the day of sampling. [H<sub>2</sub>O<sub>2</sub>] was measured at time zero and two or three other time points by sacrificing a 25-mL sealed quartz test tube with no headspace for each time point. The test tubes were submerged in about 2 cm of circulating surface seawater. Net H<sub>2</sub>O<sub>2</sub> photoproduction rates in filtered and unfiltered samples were indistinguishable. Absorbance spectra were measured with an ultraviolet-visible spectrometer back in the lab using filtered, frozen samples from these stations, which were fully thawed before measurement.

*24-h average photochemical H<sub>2</sub>O<sub>2</sub> production in the top 50 m*—To determine the 24-h average photochemical H<sub>2</sub>O<sub>2</sub> contribution over the top 50 m, P<sub>photo,50 m</sub>, we assumed that all incident photons were absorbed in the top 50 m and

calculated the production rate using Eq. 1.

$$P_{\text{photo},50\text{ m}} = \frac{W(24\text{h}, \lambda)\Phi(\lambda)}{z} \quad (1)$$

We used average wavelength ( $\lambda$ )-dependent apparent quantum yields for H<sub>2</sub>O<sub>2</sub> photoproduction ( $\Phi(\lambda)$ ) from multiple marine and fresh waters (best-fit line from Yocis et al. [2000]). Twenty-four-hour irradiance values ( $W(24\text{h}, \lambda)$ ) were calculated by integrating the sum of diffuse and direct irradiation at 1-h intervals between 298 nm and 450 nm at 55°N latitude for 30 August 2007 (National Center for Atmospheric Research [NCAR] website total ultraviolet [TUV] calculator). Using a depth ( $z$ ) of 50 m, we obtain a P<sub>photo,50 m</sub> of 0.2 nmol L<sup>-1</sup> h<sup>-1</sup>.

*Evaluation of H<sub>2</sub>O<sub>2</sub> quantum yields for the GoA*—To evaluate whether the average apparent quantum yields used above are realistic for GoA, we also calculated the expected photochemical H<sub>2</sub>O<sub>2</sub> production rate at the surface and compared it to the rate observed in ship-deck irradiations of two water samples over a mostly sunny afternoon. The expected near-surface photoproduction rate was calculated assuming optically thin conditions using Eq. 2 (adapted from Schwarzenbach et al. 1993).

$$P_{\text{surface}} = 2.3\alpha(\lambda)\Phi(\lambda)[W_{\text{direct}}(\lambda)D_{\text{direct}} + W_{\text{indirect}}(\lambda)D_{\text{indirect}}] \quad (2)$$

We used direct and indirect irradiance [ $W_{\text{direct}}(\lambda)$  and  $W_{\text{indirect}}(\lambda)$ ] values averaged over the time span of the ship-deck irradiations for a sunny day in August (NCAR website TUV calculator), the measured absorbance spectra of the samples ( $\alpha(\lambda)$  cm<sup>-1</sup>), and a distribution coefficient of 2.5 for direct light ( $D_{\text{direct}}$ , derived from the midafternoon solar zenith angle) and 1.2 for diffuse light ( $D_{\text{indirect}}$ ). The calculated photochemical production rate (45 nmol L<sup>-1</sup> h<sup>-1</sup>) was about twice the measured photochemical production rate ( $\sim 20$  nmol L<sup>-1</sup> h<sup>-1</sup>) in both samples (data not shown). The calculated value is expected to be somewhat high, because it neglects any effects of surface reflection and clouds. Thus, the quantum yields used for the calculation of P<sub>photo,50 m</sub> appear to be a reasonable estimate.

The high rate of surface photoproduction is not inconsistent with our calculated average over 50 m of the water column, because the rate decreases steeply with water depth due to light attenuation. To demonstrate this, we can estimate the rate of photoproduction in a thin film of water at depth  $z$  by using the direct and indirect irradiance values at depth  $z$ ,  $W_{\text{direct},z}(\lambda)$  and  $W_{\text{indirect},z}(\lambda)$ , in place of the  $W_{\text{direct}}(\lambda)$  and  $W_{\text{indirect}}(\lambda)$  values in Eq. 2.  $W_{\text{direct},z}(\lambda)$  and  $W_{\text{indirect},z}(\lambda)$  can be estimated as

$$W_{\text{direct},z}(\lambda) = [W_{\text{direct}}(\lambda)][10^{-\alpha(\lambda)D_{\text{direct}}z}] \quad (3)$$

$$W_{\text{indirect},z}(\lambda) = [W_{\text{indirect}}(\lambda)][10^{-\alpha(\lambda)D_{\text{indirect}}z}] \quad (4)$$

For a depth of 1 m and the near-surface  $W$  and  $D$  values discussed in the previous paragraph, we calculate that mid-afternoon photoproduction is already attenuated  $\sim 60\%$ ,

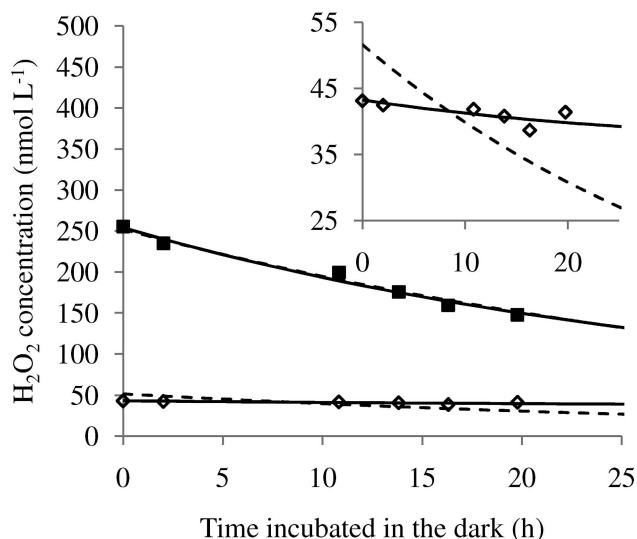


Fig. 1. Comparison of model fits of a set of dark incubations from one station (solid squares: spiked incubation; open diamonds: unaltered incubation). Solid lines show our model, with the same  $k_{\text{loss,H}_2\text{O}_2}$  ( $0.033 \text{ h}^{-1}$ ) and  $P_{\text{H}_2\text{O}_2}$  ( $1.2 \text{ nmol L}^{-1} \text{ h}^{-1}$ ) values for both incubations, while dashed lines show the best fit using  $k_{\text{loss,H}_2\text{O}_2}$  ( $0.026 \text{ h}^{-1}$ ) only.  $[\text{H}_2\text{O}_2]_0$  of each incubation was also a fitting parameter.

compared to the near-surface value. We conclude that our estimate of  $P_{\text{photo},50 \text{ m}}$  is consistent with our surface-production rate measurement.

## Results

*Validation of methodology for measuring dark production rates of  $\text{H}_2\text{O}_2$* —Absolute rates of  $\text{H}_2\text{O}_2$  decay and dark production were determined by modeling the observed  $[\text{H}_2\text{O}_2]$  vs. time in dark incubations of water samples. We assumed that  $k_{\text{loss,H}_2\text{O}_2}$  ( $\text{h}^{-1}$ ), the pseudo-first-order rate coefficient of decay, and  $P_{\text{H}_2\text{O}_2}$  ( $\text{nmol L}^{-1} \text{ h}^{-1}$ ), the dark production rate, remained constant over time, and that each parameter takes on the same value in a given water sample, whether it was left unaltered or spiked with  $\text{H}_2\text{O}_2$ . Thus the change in  $[\text{H}_2\text{O}_2]$  over time in an incubation is given by

$$\text{Rate of decay} = -k_{\text{loss,H}_2\text{O}_2}[\text{H}_2\text{O}_2] \quad (5)$$

$$\text{Rate of production} = P_{\text{H}_2\text{O}_2} \quad (6)$$

$$\frac{d[\text{H}_2\text{O}_2]}{dt} = -k_{\text{loss,H}_2\text{O}_2}[\text{H}_2\text{O}_2] + P_{\text{H}_2\text{O}_2} \quad (7)$$

Integrating Eq. 7 gives  $[\text{H}_2\text{O}_2]$  as a function of time:

$$[\text{H}_2\text{O}_2] = \left( \frac{P_{\text{H}_2\text{O}_2}}{k_{\text{loss,H}_2\text{O}_2}} \right) (1 - Ae^{-k_{\text{loss,H}_2\text{O}_2}t}) \quad (8)$$

$$A = 1 - \left( \frac{k_{\text{loss,H}_2\text{O}_2}}{P_{\text{H}_2\text{O}_2}} \right) [\text{H}_2\text{O}_2]_0 \quad (9)$$

where  $[\text{H}_2\text{O}_2]_0$  is the initial concentration of  $\text{H}_2\text{O}_2$  in a given incubation.

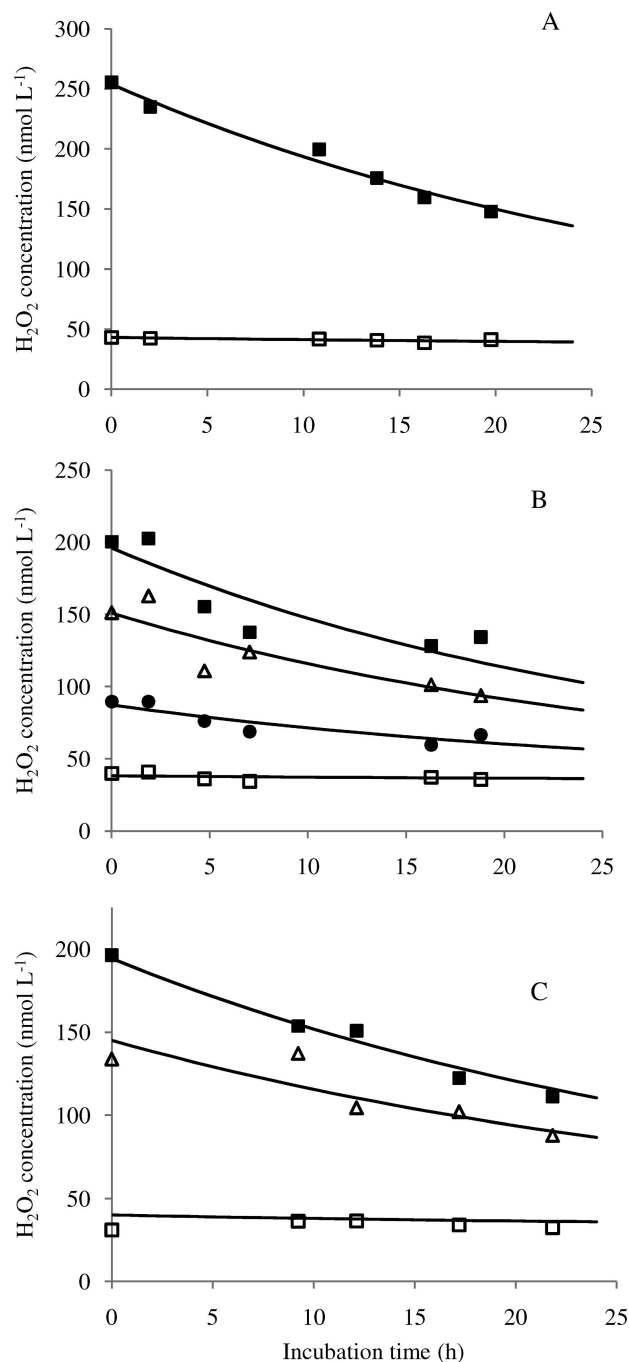


Fig. 2.  $[\text{H}_2\text{O}_2]$  vs. time during a dark incubation of a set of samples spiked with  $\text{H}_2\text{O}_2$  (diamonds, closed squares, and triangles) and left unaltered (open squares) from 10 m at Sta. (A) Kodiak 21, (B) Kodiak 24, and (C) Kodiak 25. Model fits using the same  $k_{\text{loss,H}_2\text{O}_2}$  and  $P_{\text{H}_2\text{O}_2}$  values for all incubations from the same station are shown as solid lines.

To examine whether  $P_{\text{H}_2\text{O}_2}$  was essential to producing good fits, we attempted to model the incubations assuming  $P_{\text{H}_2\text{O}_2}$  equals zero and using only  $k_{\text{loss,H}_2\text{O}_2}$  and the  $[\text{H}_2\text{O}_2]_0$  values as fitting parameters. Best fits were determined using Microsoft Excel's Solver function to minimize the sum of the squares of the differences between the actual data and the model. The resulting models typically produced good

Table 2. Absolute  $k_{\text{loss,H}_2\text{O}_2}$  and  $P_{\text{H}_2\text{O}_2}$  as a function of initial  $[\text{H}_2\text{O}_2]$ .

Station	Absolute $k_{\text{loss,H}_2\text{O}_2}$ ( $\text{h}^{-1}$ )	$P_{\text{H}_2\text{O}_2}$ ( $\text{nmol L}^{-1} \text{h}^{-1}$ )	$[\text{H}_2\text{O}_2]_0$ ( $\text{nmol L}^{-1}$ )
Kodiak 22	—	—	58*
	0.019	1.0	132
	0.033	1.7	192
Kodiak 24	—	—	40*
	0.040	1.4	90
	0.039	1.3	151
	0.034	1.2	200
Kodiak 25	—	—	31*
	0.026	0.9	134
	0.034	1.2	196
Kodiak 27	—	—	70*
	0.026	1.9	159
	0.018	1.3	224

\* Unaltered sample used to model each spiked incubation.

fits of the spiked incubations, but the unaltered incubations showed much less net decay than predicted by the model (Fig. 1). In contrast, the model using  $P_{\text{H}_2\text{O}_2}$ ,  $k_{\text{loss,H}_2\text{O}_2}$  and the  $[\text{H}_2\text{O}_2]_0$  values as the fitting parameters provided good fits for all incubations (Fig. 2 shows 3 stations).

For those samples incubated with several  $\text{H}_2\text{O}_2$  spikes, there was no observable trend in  $k_{\text{loss,H}_2\text{O}_2}$  or  $P_{\text{H}_2\text{O}_2}$  as a function of  $\text{H}_2\text{O}_2$  spike concentration (Table 2), lending support to our assumption that these parameters are unchanged by the spike additions. It has previously been observed that biological decay can be fit as a pseudo-first-order rate, with  $k_{\text{loss,H}_2\text{O}_2}$  independent of the initial  $[\text{H}_2\text{O}_2]$  (Cooper et al. 1994; Wong et al. 2003). Because the decay coefficient is dependent on the health, characteristics, and cell concentration of the biological community in the sample (Yuan and Shiller 2001; Richard et al. 2007), experiments were conducted for fewer than 24 h to minimize the chance for a change in kinetics due to alterations in the community. No systematic divergences of model from data were observed over 24 h, indicating that no dramatic changes in  $k_{\text{loss,H}_2\text{O}_2}$  or  $P_{\text{H}_2\text{O}_2}$  took place over that time span.

Uncertainties in the parameters  $P_{\text{H}_2\text{O}_2}$  and  $k_{\text{loss,H}_2\text{O}_2}$  were determined by fitting a single spiked sample with the unaltered sample, obtaining the values, and then fitting a second spiked sample with the same unaltered sample to compare the results. Analysis of error in this manner from four different 10-m samples resulted in an average error of 23% for both  $P_{\text{H}_2\text{O}_2}$  and  $k_{\text{loss,H}_2\text{O}_2}$ , where each variable ranged from 1.1  $\text{nmol L}^{-1} \text{h}^{-1}$  to 1.9  $\text{nmol L}^{-1} \text{h}^{-1}$  and 0.018  $\text{h}^{-1}$  to 0.036  $\text{h}^{-1}$ , respectively (Table 2). Individual errors were estimated as either the average standard deviation of 0.3  $\text{nmol L}^{-1} \text{h}^{-1}$  and 0.006  $\text{h}^{-1}$  for  $P_{\text{H}_2\text{O}_2}$  and  $k_{\text{loss,H}_2\text{O}_2}$ , respectively, or 23% error, whichever was greater. Because it is easier to measure and fit larger changes in  $\text{H}_2\text{O}_2$  concentration, our method produces the best results in samples with net decay coefficients for spiked samples greater than about 0.005  $\text{h}^{-1}$ . In the filtered controls, initial concentrations ranged from 45  $\text{nmol L}^{-1}$  to 145  $\text{nmol L}^{-1}$  and  $[\text{H}_2\text{O}_2]$  changed very little ( $+2 \pm 4 \text{ nmol L}^{-1}$  over the course of 24 h), probably due to contamination from air. This equates to an average production rate of about 0.09  $\text{nmol L}^{-1} \text{h}^{-1}$ , which is small compared to the dark production rates we measured in unfiltered samples.

The  $\text{H}_2\text{O}_2$  decay rate coefficients measured in our study lie within the range determined throughout the world's oceans (Table 3); however, our decay rate coefficients represent absolute values rather than the net values reported by all but one of these previous studies (Moffett and Zafiriou 1990). We observed that net decay coefficients underestimated the absolute values by as much as 50% in incubations spiked with  $\text{H}_2\text{O}_2$ , and to a much larger degree in unaltered samples (Fig. 3), where decay and production rates were often of a similar magnitude. Thus, many previous studies may also have underestimated the absolute decay constant by neglecting the dark production term in Eq. 7 and fitting the observed net decay to a pseudo-first-order curve.

*Hydrogen peroxide production rates*— $\text{H}_2\text{O}_2$  dark production rates varied widely throughout the GoA, but in general they decreased with depth in the top 50 m (Fig. 4). This depth dependence probably reflects a decrease in

Table 3. Hydrogen peroxide dark decay rate coefficients for various marine studies.

Study location	Depth (m)	$k_{\text{loss,H}_2\text{O}_2}$ ( $\text{h}^{-1}$ )	$[\text{H}_2\text{O}_2]$ after spike ( $\text{nmol L}^{-1}$ )	Reference
Vineyard Sound	surface	0.054	117–120	Moffett and Zafiriou 1990
Bermuda (BATS)	5–40	0.0075–0.0106*	120	Avery et al. 2005
Bermuda (BATS)	250	0.003*	120	Avery et al. 2005
Central Atlantic	surface	0.0054*	~80†	Yuan and Shiller 2001
Florida coastal	surface	0.006–0.058*	124–242	Petasne et al. 1997
Florida offshore	0.5–150	0.003–0.014*	124–242	Petasne et al. 1997
Gulf of Alaska	surface	0.019–0.110	100–250	This study
Gulf of Alaska	10–50	0.003–0.041	100–250	This study
NW Pacific	surface	0.004–0.009*	33–120†	Yuan and Shiller 2005
Caribbean Sea	2–40	0.006–0.122*	60–150†	Moore et al. 1993
Mediterranean Sea coast	surface	0.01–0.28*	25–800	Herut et al. 1998

\* Net decay rate, dark production not accounted for.

† No  $\text{H}_2\text{O}_2$  spike.

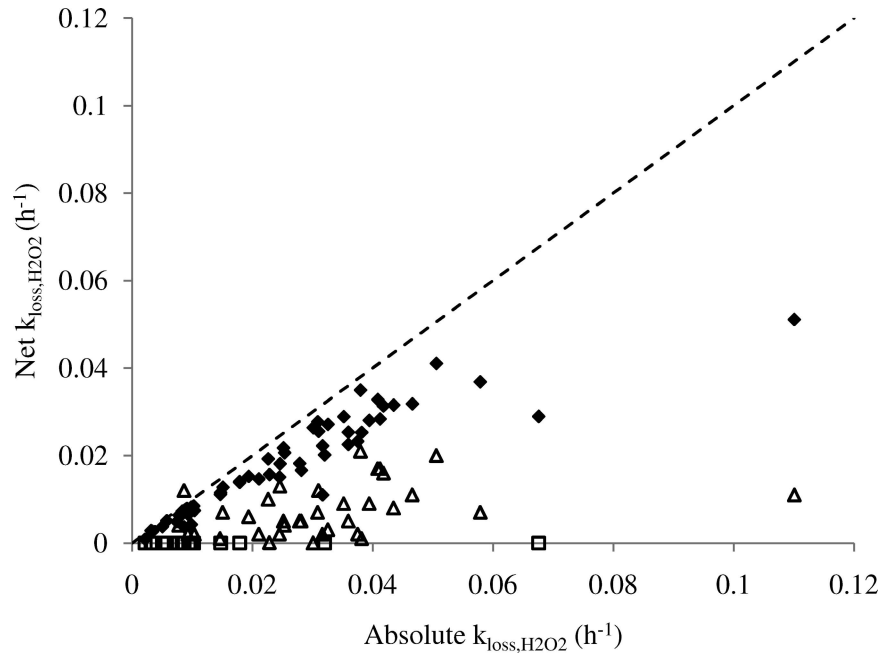


Fig. 3. Comparison of absolute decay rate coefficients determined by the model fit and net decay rate coefficients calculated from individual first-order fits of  $\text{H}_2\text{O}_2$  in spiked (filled diamonds) and unaltered (open triangles) incubations without consideration of dark production. When net production was observed instead of net decay in unaltered samples, the net decay rate coefficient was set to zero (open squares). Dashed line shows where the rate coefficients would be equal.

biological activity with depth in the GoA. Chlorophyll was typically also highest near the surface and decreased steeply below the mixed layer, whose depth ranged from 15 m to 30 m. Examining a correlation between chlorophyll and

$\text{P}_{\text{H}_2\text{O}_2}$  would be inappropriate, because significant time (2–24 h) elapsed between collection of GO-FLO samples for incubations and CTD rosette samples for chlorophyll measurements, and large variability in subsequent chloro-

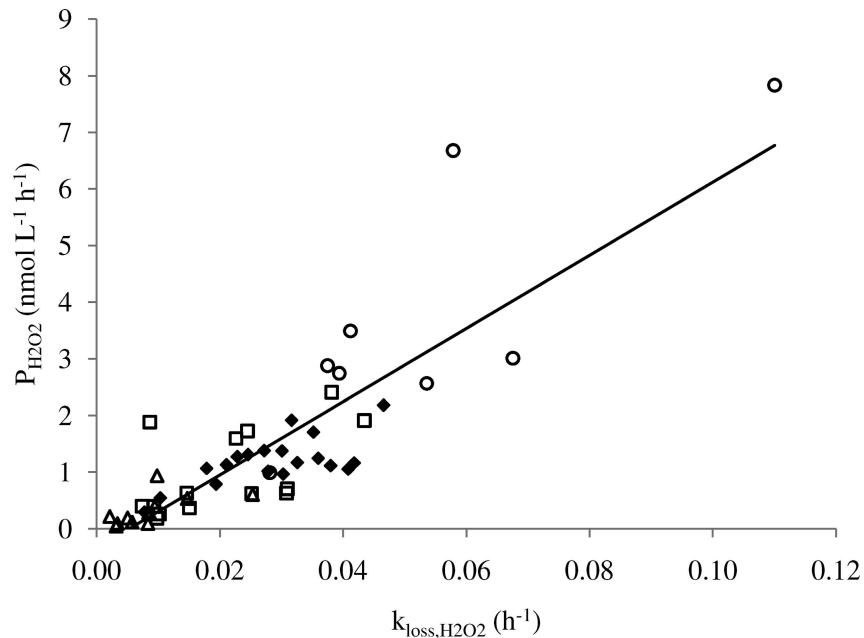


Fig. 4. Correlation between the dark biological production rate ( $\text{P}_{\text{H}_2\text{O}_2}$ ) and the decay rate coefficient ( $k_{\text{loss,H}_2\text{O}_2}$ ) at 1–6 m (circle), 10 m (diamond), 25 m (square), and 50 m (triangle). A best-fit linear regression is shown for the data where the equation of the line is  $y = 64.6x - 0.34$  ( $R^2 = 0.74$ ).

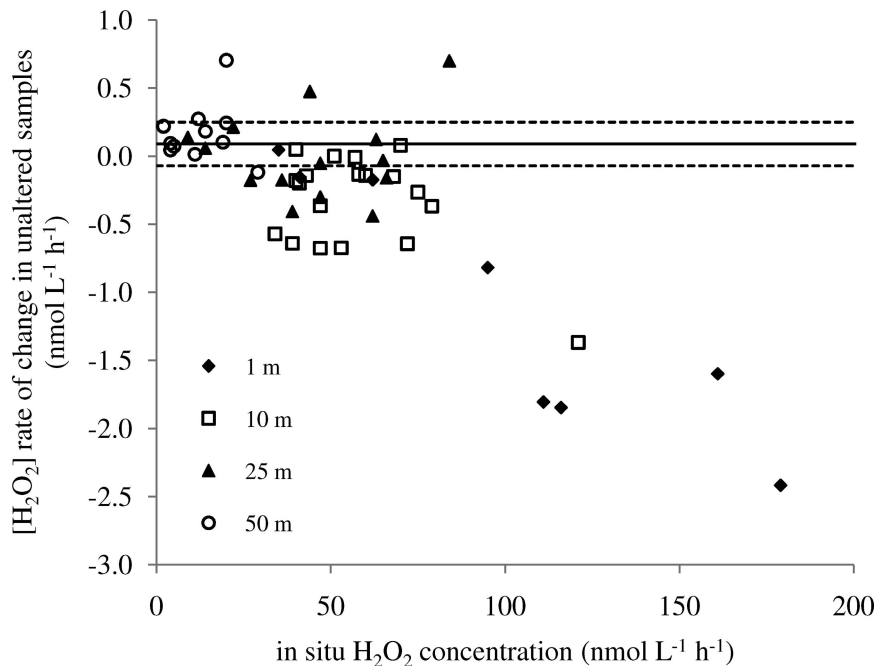


Fig. 5. The rate of change in  $[H_2O_2]$  during dark unaltered incubations (diamonds), obtained from linear regressions of  $[H_2O_2]$  vs. time, is shown as a function of the initial in situ  $[H_2O_2]$ . The uncertainty of these points, assessed as one standard deviation of each regression slope, is 0.23 and 0.13 for slope values  $<$ , and  $>$  an  $-0.5 \text{ nmol L}^{-1} \text{ h}^{-1}$ , respectively. Horizontal lines show the average rate of change for filtered controls (solid line) with the 95% confidence interval (dashed lines),  $n = 7$ .

phyll profiles was observed on these time scales. There is a good correlation between the decay rate coefficients, which are recognized to be biologically mediated (Cooper et al. 1994), and the rates of dark production (Fig. 4;  $R^2 = 0.74$ ).

*Photochemical vs. dark production*—To compare the relative importance of photochemical vs. biological  $H_2O_2$  sources, we estimated the total dark  $H_2O_2$  contribution as follows: we assumed that biological production was constant throughout the day and fit the median  $P_{H_2O_2}$  values from 1 m, 10 m, 25 m, and 50 m to an exponential function ( $R^2 > 0.99$ ) of  $P_{H_2O_2}$  vs. depth. This function was then used to calculate an average from 0 m to 50 m,  $P_{H_2O_2,50 \text{ m}}$ , of  $0.8 \text{ nmol L}^{-1} \text{ h}^{-1}$ . We can compare this to  $0.2 \text{ nmol L}^{-1} \text{ h}^{-1}$ , the photochemical  $H_2O_2$  production rate over the top 50 m,  $P_{\text{photo},50 \text{ m}}$ , calculated in the Method section (*24-h average photochemical  $H_2O_2$  production in the top 50 m*). Although the exact ratio of  $P_{H_2O_2,50 \text{ m}}$  to  $P_{\text{photo},50 \text{ m}}$  will vary greatly in the GoA for any one location and time, we conclude that dark production is a significant contributor to the  $H_2O_2$  budget of the GoA.

This comparison assumes that biological production rates are constant throughout the course of the day. The dark values we measured could underestimate daytime biological production, because incomplete oxidation of water during photosynthesis can lead to  $H_2O_2$  production within the cell; however, it is unclear whether this  $H_2O_2$  can diffuse from the cell and contribute to the measured production rate in the surrounding water. We did not observe any difference in the  $H_2O_2$  photochemical produc-

tion rate in filtered and unfiltered irradiations at two different stations (data not shown).

We also compared dark and photochemical production by observing whether  $[H_2O_2]$  decreases over time in unaltered incubations, which would indicate an initial excess over the steady state  $[H_2O_2]$  one would expect from dark (presumably photochemical) production and decay. Eighty-eight percent of the surface ( $n = 8$ ), 79% of the 10 m ( $n = 19$ ), 43% of the 25 m ( $n = 14$ ), and 8% of the 50 m ( $n = 12$ ) incubations showed net decay in excess of the 95% confidence interval of the filtered controls (data points below the bottom dashed line in Fig. 5), indicating that the majority of the incubations of the deeper samples began with  $[H_2O_2]$  close to the expected dark steady state. In general, the larger net  $[H_2O_2]$  decay rates were associated with larger in situ  $[H_2O_2]$  ( $> 75 \text{ nmol L}^{-1}$ ). A few of the deeper samples showed a net increase in  $[H_2O_2]$  over time (data points above the top dashed line in Fig. 5), perhaps reflecting an increase in biological activity as these samples were incubated at warmer surface water temperatures.

## Discussion

Our work presents the strongest evidence to date of the importance of dark (presumably biological) production of  $H_2O_2$  in the Pacific, as hypothesized by Yuan and Shiller (2005). The major source of  $H_2O_2$  in the ocean has typically been assumed to be abiotic photochemical production in the near-surface, with mixing processes transporting the photochemical signature to greater depths. Our finding that

[H<sub>2</sub>O<sub>2</sub>] concentrations are near the dark steady state in most of the deeper samples suggests that the [H<sub>2</sub>O<sub>2</sub>] at those depths could be maintained primarily by dark production instead.

It is possible that extracellular H<sub>2</sub>O<sub>2</sub> is a common byproduct of biological processes (as is intracellular H<sub>2</sub>O<sub>2</sub>), and that the large spatial variability in H<sub>2</sub>O<sub>2</sub> production rates that we observed merely reflects variability in general biological activity at this field site. Alternatively, H<sub>2</sub>O<sub>2</sub> may be a product of a specific biochemical process, which might mean that production rates will vary with environmental factors and species composition. Further work is needed to distinguish between these possibilities and to determine the relationship between biological production of hydrogen peroxide and superoxide.

#### Acknowledgments

Thanks to the captain and crew of the R/V *Thomas G. Thompson* for support during the cruise and chief scientist Ken Bruland for giving us the opportunity to participate. Ken Bruland, Maeve Lohan, Geoff Smith, and Matt Brown provided excellent advice and assisted with sample collection. Jed Goldstone made us aware of the National Center for Atmospheric Research irradiance data. The insightful comments of Alan Shiller and an anonymous reviewer were very helpful in preparation of this manuscript. Funding for this work was provided by a National Science Foundation grant from the division of Ocean Sciences 0551715, a fellowship from the Denver chapter of Achievement Rewards for College Scientists (ARCS), and an Erickson scholarship.

#### References

- EVERY, G. B., W. J. COOPER, R. J. KIEBER, AND J. D. WILLEY. 2005. Hydrogen peroxide at the Bermuda Atlantic Time Series Station: Temporal variability of seawater hydrogen peroxide. *Mar. Chem.* **97**: 236–244.
- COOPER, W. J., J. K. MOEGLING, R. J. KIEBER, AND J. J. KIDDLE. 2000. A chemiluminescence method for the analysis of H<sub>2</sub>O<sub>2</sub> in natural waters. *Mar. Chem.* **70**: 191–200.
- , C. W. SHAO, D. R. S. LEAN, A. S. GORDON, AND F. E. SCULLY. 1994. Factors affecting the distribution of H<sub>2</sub>O<sub>2</sub> in surface waters, p. 391–422. *In* L. A. Baker [ed.], *Environmental chemistry of lakes and reservoirs*. American Chemical Society.
- HERUT, B., E. SHOHAM-FRIDER, N. KRESS, U. FIEDLER, AND D. L. ANGEL. 1998. Hydrogen peroxide production rates in clean and polluted coastal marine waters of the Mediterranean, Red and Baltic Seas. *Mar. Pollut. Bull.* **36**: 994–1003.
- JOHNSON, K. S., S. W. WILLASON, D. A. WIESENBERG, S. E. LOHRENZ, AND R. A. ARNONE. 1989. Hydrogen peroxide in the western Mediterranean Sea: A tracer for vertical advection. *Deep-Sea Res.* **36**: 241–254.
- KIM, D., AND OTHERS. 2000. Mechanism of superoxide anion generation in the toxic red tide phytoplankton *Chattonella marina*: Possible involvement of NAD(P)H oxidase. *Biochim. Biophys. Acta* **1524**: 220–227.
- KING, D. W., AND OTHERS. 2007. Flow injection analysis of H<sub>2</sub>O<sub>2</sub> in natural waters using acridinium ester chemiluminescence: Method development and optimization using a kinetic model. *Anal. Chem.* **79**: 4169–4176.
- KUSTKA, A. B., Y. SHAKED, A. J. MILLIGAN, D. W. KING, AND F. M. M. MOREL. 2005. Extracellular production of superoxide by marine diatoms: Contrasting effects on iron redox chemistry and bioavailability. *Limnol. Oceanogr.* **50**: 1172–1180.
- MARSHALL, J. A., M. DE SALAS, T. ODA, AND G. HALLEGRAEFF. 2005. Superoxide production by marine microalgae. *Mar. Biol.* **147**: 533–540.
- MICINSKI, E., L. A. BALL, AND O. C. ZAFIRIOU. 1993. Photochemical oxygen activation: Superoxide radical detection and production rates in the eastern Caribbean. *J. Geophys. Res. Oceans* **98**: 2299–2306.
- MILLER, G. W., AND OTHERS. 2005. Hydrogen peroxide method intercomparison study in seawater. *Mar. Chem.* **97**: 4–13.
- MILLERO, F. J., AND S. SOTOLONGO. 1989. The oxidation of Fe(II) with H<sub>2</sub>O<sub>2</sub> in seawater. *Geochim. Cosmochim. Acta* **53**: 1867–1873.
- MOFFETT, J. W., AND O. C. ZAFIRIOU. 1990. An investigation of hydrogen peroxide chemistry in surface waters of Vineyard Sound with H<sub>2</sub><sup>18</sup>O<sub>2</sub> and <sup>18</sup>O<sub>2</sub>. *Limnol. Oceanogr.* **35**: 1221–1229.
- , AND R. G. ZIKA. 1987. Reaction kinetics of hydrogen peroxide with copper and iron in seawater. *Environ. Sci. Technol.* **21**: 804–810.
- MOORE, C. A., C. T. FARMER, AND R. G. ZIKA. 1993. Influence of the Orinoco River on hydrogen peroxide distribution and production in the eastern Caribbean. *J. Geophys. Res. Oceans* **98**: 2289–2298.
- OBERNOSTERER, I., P. RUARDIJ, AND G. J. HERNDL. 2001. Spatial and diurnal dynamics of dissolved organic matter (DOM) fluorescence and H<sub>2</sub>O<sub>2</sub> and the photochemical oxygen demand of surface water DOM across the subtropical Atlantic Ocean. *Limnol. Oceanogr.* **46**: 632–643.
- PALENIK, B., AND F. M. M. MOREL. 1988. Dark production of H<sub>2</sub>O<sub>2</sub> in the Sargasso Sea. *Limnol. Oceanogr.* **33**: 1606–1611.
- , O. C. ZAFIRIOU, AND F. M. M. MOREL. 1987. Hydrogen peroxide production by a marine phytoplankter. *Limnol. Oceanogr.* **32**: 1365–1369.
- PETASNE, R. G., AND R. G. ZIKA. 1987. Fate of superoxide in coastal seawater. *Nature* **325**: 516–518.
- , AND ———. 1997. Hydrogen peroxide lifetimes in south Florida coastal and offshore waters. *Mar. Chem.* **56**: 215–225.
- PETTINE, M., F. GENNARI, L. CAMPANELLA, AND F. J. MILLERO. 2008. The effect of organic compounds in the oxidation kinetics of Cr(III) by H<sub>2</sub>O<sub>2</sub>. *Geochim. Cosmochim. Acta* **72**: 5692–5707.
- PRICE, D., R. FAUZI, C. MANTOURA, AND P. J. WORSFOLD. 1998. Shipboard determination of hydrogen peroxide in the western Mediterranean sea using flow injection with chemiluminescence detection. *Anal. Chim. Acta* **377**: 145–155.
- RICHARD, L. E., B. M. PEAKE, S. A. RUSAK, W. J. COOPER, AND D. J. BURRITT. 2007. Production and decomposition dynamics of hydrogen peroxide in freshwater. *Environ. Chem.* **4**: 49–54.
- ROSE, A. L., J. W. MOFFETT, AND T. D. WAITE. 2008a. Determination of superoxide in seawater using 2-methyl-6-(4-methoxyphenyl)-3,7-dihydroimidazo[1,2-a]pyrazin-3(7H)-one chemiluminescence. *Anal. Chem.* **80**: 1215–1227.
- , T. P. SALMON, T. LUKONDEH, B. A. NEILAN, AND T. D. WAITE. 2005. Use of superoxide as an electron shuttle for iron acquisition by the marine cyanobacterium *Lyngbya majuscula*. *Environ. Sci. Technol.* **39**: 3708–3715.
- , E. A. WEBB, T. D. WAITE, AND J. W. MOFFETT. 2008b. Measurement and implications of nonphotochemically generated superoxide in the equatorial Pacific Ocean. *Environ. Sci. Technol.* **42**: 2387–2393.
- SCHWARZENBACH, R. P., P. M. GSCHWEND, AND D. M. IMBODEN. 1993. *Environmental organic chemistry*. Wiley.
- SUNDA, W. G., AND S. A. HUNTSMAN. 1994. Photoreduction of manganese oxides in seawater. *Mar. Chem.* **46**: 133–152.

- VERMILYEA, A. W. 2009. Hydrogen peroxide in natural waters. Ph.D. thesis. Colorado School of Mines.
- WONG, G. T. F., W. M. DUNSTAN, AND D. KIM. 2003. The decomposition of hydrogen peroxide by marine phytoplankton. *Oceanologica Acta* **26**: 191–198.
- YOCIS, B. H., D. J. KIEBER, AND K. MOPPER. 2000. Photochemical production of hydrogen peroxide in Antarctic Waters. *Deep-Sea Res. I* **47**: 1077–1099.
- YUAN, J. C., AND A. M. SHILLER. 1999. Determination of subnanomolar levels of hydrogen peroxide in seawater by reagent-injection chemiluminescence detection. *Anal. Chem.* **71**: 1975–1980.
- , AND ———. 2001. The distribution of hydrogen peroxide in the Southern and central Atlantic Ocean. *Deep-Sea Res. II* **48**: 2947–2970.
- , AND ———. 2004. Hydrogen peroxide in deep waters of the North Pacific Ocean. *Geophys. Res. Lett.* **31**: L01310, doi:10.1029/2003GL018439.
- , AND ———. 2005. Distribution of hydrogen peroxide in the northwest Pacific Ocean. *Geochem. Geophys. Geosystems* **6**: Q09M02, doi:10.1029/2004GC000908.

*Associate editor: Mary I. Scranton*

*Received: 09 June 2009*  
*Accepted: 02 November 2009*  
*Amended: 12 November 2009*